



## Air-Breathing Electric Propulsion for Long-Term Flights in Very Low Earth Orbits

A.I. Erofeev<sup>1</sup>, A.S. Filatyev<sup>1</sup>, A.A. Golikov<sup>1</sup>, S.A. Khartov<sup>2</sup>, A.P. Nikiforov<sup>1</sup>, G.A. Popov<sup>2</sup>, M.O. Suvorov<sup>2</sup>,  
O.V. Yanova<sup>1</sup>

### Abstract

The paper presents the results of solving a number of problems for the practical implementation of the concept of air-breathing electric propulsion (ABEP) using gases of the surrounding atmosphere as a propellant. Conditions for long term existence of spacecraft (SC) with ABEP in low Earth orbits, including areas of preferable using the ABEP as compared to traditional electric propulsion, were determined in terms of generalized parameters, combining characteristics of SC, ABEP, power sources and target orbits. On the basis of the developed physic-mathematical model of mass transfer processes the possibility of creating a working gas density in the ABEP ionization chamber, hundreds of times greater than the density of the environment, is shown. A developed laboratory model of the ABEP thrust unit according to the radio-frequency ion thruster scheme is presented. The synthesis of the optimal control of the ABEP thrust vector was obtained for SC maintenance in a given orbit and the fastest change of orbit's parameters (apogee altitude and orbit inclination).

**Keywords:** *air-breathing electric propulsion, spacecraft, optimal control*

### 1. Introduction

Reducing the orbit's altitude of prospective monitoring spacecraft (SC) can significantly improve the efficiency of its onboard recording equipment. However such altitude reducing, taking into account the orbital SC velocity and atmospheric gases, creates an aerodynamic drag, which leads to a further orbital altitude decrease, significantly limiting the SC lifetime. For increasing the SC lifetime such aerodynamic drag should be compensated by the power plant (PP) thrust. The experience of long-term operation (over 4 years) of the *GOCE* [1] SC of European Space Agency in orbits of 250-280 km is known. The orbit altitude of this SC was maintained and corrected by the electric propulsion (EP) of *QinetiQ*. SC ceased its existence upon completion of the 40 kg of Xenon stored on board.

Currently EP are widely used in orbit correction systems of a number of SC [2]. The experience of their operation indicates the feasibility of using EP for low-orbital SC with enhanced lifetime [3]. One of the factors, significantly preventing the reduction of the orbit altitude and the increase of lifetime of SC with EP, is the need to take on board the working gas (WG), the mass consumption of which increases exponentially with decreasing the flight altitude. This limitation can be overcome by taking the WG from the atmosphere SC surrounding. Such an opportunity is provided by air-breathing electric propulsion (ABEP).

The idea to use atmospheric gases from the Earth's upper atmosphere as a propellant has long been discussed [5], [6]. Nowadays, studies of the possibility of creating ABEP continue both in Russia and abroad [7] - [15].

The relevance of the research is based on the increasing interest shown in recent years in low orbits for locating SC constellations. On the obvious advantages of low orbits, the following facts say: with decreasing altitude  $h$ , if other conditions are constant, the desired power of the communication hardware decreases in proportion to  $h^2$ , the resolution of the optical system improves proportionally to  $h$ . Today such global projects as SpaceX, OneWeb, etc. are being implemented to replace heavy

<sup>1</sup> Central Aerohydrodynamic Institute, Zhukovsky, Moscow region, Russia, [filatyev@yandex.ru](mailto:filatyev@yandex.ru)

<sup>2</sup> Research Institute of Applied Mechanics and Electrodynamics of Moscow Aviation Institute (RIAME MAI), Moscow, Russia, [riame@sokol.ru](mailto:riame@sokol.ru)

satellites in geostationary orbits by constellations of small-satellite (weighing 150-450 kg) in low Earth orbits of ~ 1000 km altitude.

For example, in comparison with low orbits of altitude of ~ 1000 km with everything else being equal, it is possible

Transition to ultra-low orbits of altitude of 150-200 km for SC equipped PVERD being developed will allow: to reduce the SC mass by 60 to 300 times, the satellite receiver power by 15 to 50 times; to increase the resolution of the optical system in 4 - 7 times; to reduce the dispersion and delay of the signal.

For the practical implementation of the ABEP concept it is necessary to ensure

- the accumulation of a sufficient mass of gas from the rare ambient atmosphere [12];
- a sufficient impulse to the accumulated gas and necessary power supply for such ABEP [15];
- the optimal control of ABEP, the power supply source (depending on its type) and the SC orientation (which affects the aerodynamic drag and, with the use of solar arrays, the rate of energy storage) [13, 14];
- thermal fluxes, admissible for long-term SC lifetime in the ultra-low orbits [15].

Experimental studies [8, 12] have confirmed adequacy of the physic-mathematical model of mass transfer processes, developed on the basis of the concept of diffuse reflection of molecules from the surface for ABEP air intakes of various shapes. It is shown that the WG density in the ABEP thermalizer can be made in two or three orders greater than the atmosphere density.

Parameters characterizing the feasibility conditions of SC with ABEP, such as the SC shape, permissible thermal fluxes, available electric power, WG mass and ABEP efficiency, and orbit parameters, are combined into two generalized parameters. The regions of existence of the ultralow-orbit SC with ABEP in terms of these generalized parameters are determined. The investigation of ER applicability to maintain SC in low and ultralow orbits has been carried out. In coordinates of SC lifetime and orbit altitude the evaluation of regions of preferable using ABEP in comparison with EP was made depending on parameters of SC, engines and power plants [14].

The synthesis of the optimal control of the ABEP thrust vector to maintain SC at a given low orbit and to provide the fastest change of orbit parameters (apogee altitude and inclination) was obtained taking into account constraints on the thrust and power of energy source [13].

## 2. Operating scheme of ABEP

ABEP generally includes (Fig. 1): air intake (1), ensuring the collection of atmospheric gases; a thermalizer (2), in which the gas particles are decelerated to small (thermal) velocities; ionization chamber (3), in which the gas is ionized; acceleration region (4), in which the ionized gas accelerates by an electromagnetic field; and a neutralizer (5) of an ejected plasma jet. The functioning of systems 3-5 requires a power source (PS), as which a solar cell battery can be used.

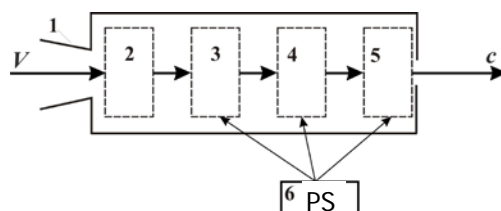


Fig. 1. Operating scheme of ABEP

### 3. Spacecraft low-orbiting conditions

Conditions for the long-term maintenance of spacecraft with electric ramjet on ultralow orbits are derived from the momentum conservation law taking into account constraints on power plant (PP) power and thermal flux. The following assumptions are made:

- the SC sectional area is equal to the intake inlet  $S_{in}$ ,
- the SC length compared to the characteristic size of the intake can be neglected,
- the dependence of the orbital velocity  $V$  on the orbit altitude  $h$  is negligible compared to the exponential dependence of the atmosphere density  $\rho(h)$ .

In view of the accepted assumptions the level lines of the minimum allowable orbit altitude  $h_{min}$  are constructed on the plane of parameters  $lg w$  and  $lg \bar{q}$ , characterizing PP power  $W_p$  and maximum admissible thermal flux  $q_{adm}$  (Fig. 2), where  $\bar{q} = q_{adm}/q_*$ ,  $q_*$  is the thermal flux at a certain characteristic circular orbit (CCO) with radius  $R_*$  and altitude  $h_*$ ,  $w = 2\eta k_1 \bar{W}_p$ ,  $\eta$  is the ABEP efficiency factor,  $0 \leq k_1 \leq 1$  is the WG mass utilization factor,  $\bar{W}_p = W_p/W_*$ ,  $W_p = 0.5 S_{in} \rho V^3 / (\eta k_1)$ ,  $W_* = \rho(h_*) S_{in} V_*^3$ .

Using obtained dependencies the minimum-altitude circular orbits are derivable for the long-term operation of the ABEP-powered SC with an assigned power. Thus with  $W_p = 500$  W,  $S_{in} = 1$  m<sup>2</sup>,  $\eta = k_1 = 0.9$ , we obtain  $lg w = -2.52$  and find  $h_{min} = 155$  km from Fig. 2. Inversely, derivable is the power necessary to maintain the SC assigned orbit parameter, for example for  $h_{min} = 120$  km it follows from Fig. 2  $lg w = -1.42$  and then determine the required power for the same flight conditions  $W_p = 6.3$  kW, which is an order higher than the value of the previous example with the orbit altitude of 155 km.

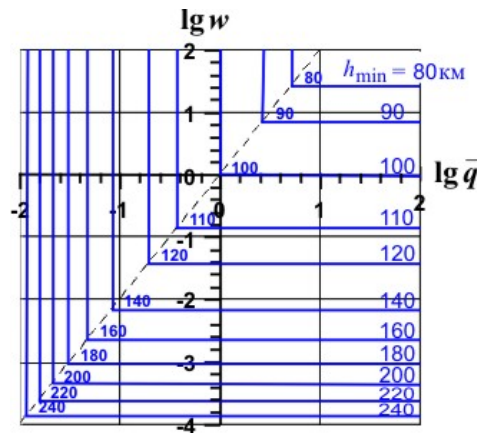


**Fig. 2.** SC orbit minimum radius lines on the plane of parameters  $lg w$  and  $lg \bar{q}$ , characterizing PS power  $W_p$  and maximum admissible thermal flux

### 4. Research of the gas flow through the air intake

To ensure the guaranteed maintenance of the SC at a given altitude, the engine must have a thrust of at least the maximum value of aerodynamic resistance at the maximum of solar and geomagnetic activity. The possibility of maintaining the low-orbit SC with ABEP was considered in [7].

Studies of air intakes operating in the upper atmosphere under conditions of a free-molecular flow are mainly carried out under the assumption of diffuse reflection of gas molecules from the surfaces of intake channel and the thermalizer [12], [13].

To study the physical processes associated with the boundary conditions when molecules are reflected from the surface, a simple scheme of the air intake using a single channel is considered (Fig. 3).

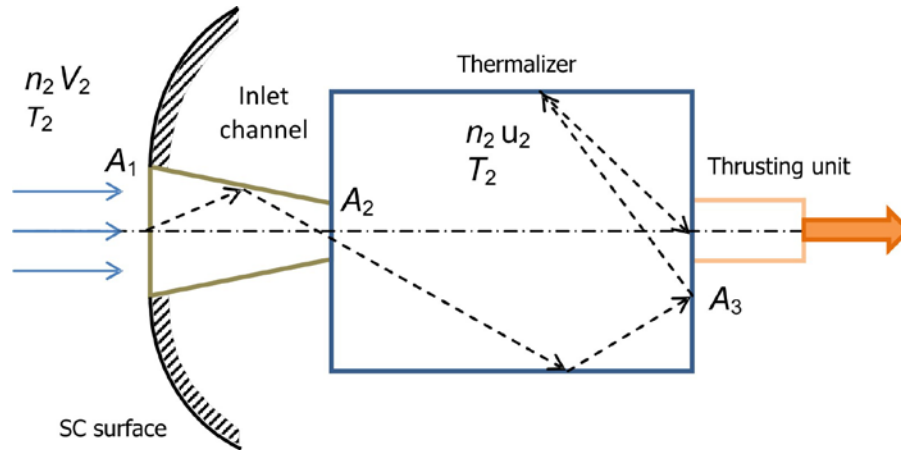


**Fig. 3.** A schematic diagram of ABEP (the dotted line shows the possible trajectories of the molecules of the outer atmosphere)

When the vehicle moves with a velocity  $V_\infty$ , the gas from the atmosphere (with a density  $n_\infty$ ) is captured by the intake and then passes to the thermalizer (directly or after several collisions with the channel walls), where the gas thermalizes, that is acquires the Maxwell distribution at the temperature  $T_2$  (the most probable velocity of molecules at this temperature is  $u_2$ ). Some part of the gas returns to the atmosphere through the intake channel, and the other part of the gas can be used as the propellant in the thrust unit. Because of the differences in the probabilities of molecule flight from the atmosphere to the thermalizer  $p_{1s}$  and from the thermalizer to the atmosphere  $p_{2d}$ , in the velocities  $V_\infty$  and  $u_2$ , and in the geometric parameters of the intake, the gas density in the thermalizer can be appreciably higher than the gas density in the atmosphere. Based on the condition of conservation of the number of particles, summarizing the fluxes of molecules entering and leaving the thermalizer, we can obtain the following equation for determining the gas density in the thermalizer  $n_2$  for the steady case:

$$p_{1s} n_\infty V_\infty A_1 - p_{2d} n_2 \frac{u_2}{2\sqrt{\pi}} A_2 - p_{3d} n_2 \frac{u_2}{2\sqrt{\pi}} A_3 = 0, \quad (1)$$

where  $A_1$  and  $A_2$  are the input and output areas of the intake, and  $A_3$  is the area of the cross section through which the gas is sampled into the thrust unit ( $p_{3d}$  is the probability of molecule passage into the thrust unit). In the absence of gas extraction from the thermalizer, the relation of the maximum density of the gas in the thermalizer  $n_{2max}$  to the gas flow density  $n_\infty$  is

$$Q_n = \frac{n_{2max}}{n_\infty} = 2\sqrt{\pi} \frac{V_\infty}{u_2} B_n, \quad B_n = \frac{p_{1s} A_1}{p_{2d} A_2}. \quad (2)$$

Fulfillment of (2) was checked experimentally depending on the gas flow rate.

Experiments aimed at determining the efficiency of air intakes in high-velocity free-molecular gas flows were performed in the VAT-103 vacuum wind tunnel in the flows of gases that are components of the atmosphere (nitrogen, a mixture of molecular and atomic oxygen, helium). All experimental studies were accompanied by Monte Carlo calculations that simulate experimental conditions.

The efficiency of air intakes was studied for three geometric shapes (cylindrical tube, tube with a square cross section, and confuser) and three types of the thermalizer: spherical, cylindrical and box-shaped alloy D16T, made of the D16T alloy. The design of the laboratory sample of the multi-channel (or honeycomb) intake was jointly developed by TsAGI and NII PME MAI. Laboratory sample is made of stainless steel and tested with box-shaped and cylindrical thermalizers (Fig. 4).

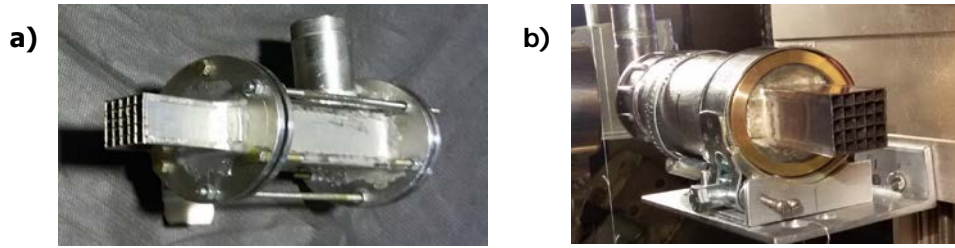


**Fig. 4.** The honeycomb intake with box-shaped (a) and cylindrical (b) thermalizers

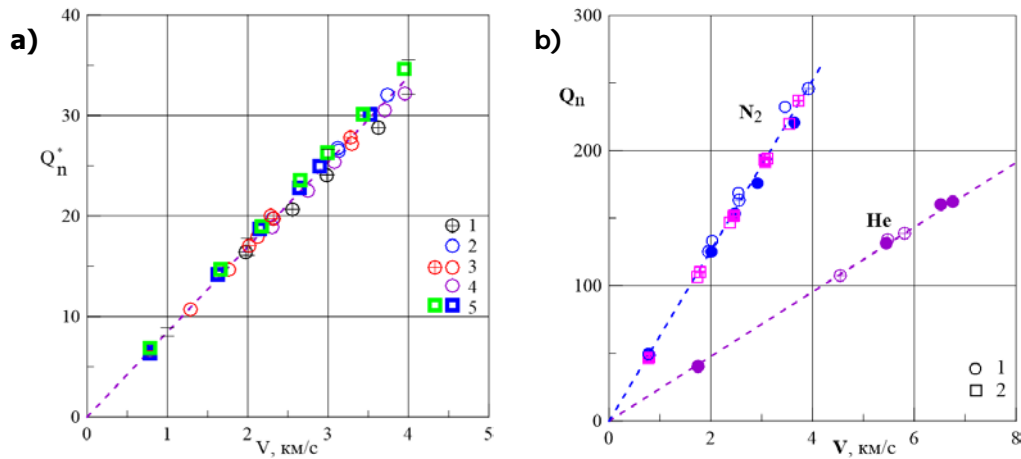


**Fig. 5.** Increase in the density of nitrogen and helium in the thermalizer of cylinder (1) and box-type shape (2). Dotted lines correspond to the calculations with a) single, and b) honeycomb intakes: a) 1-3 cylindrical tube: 1 –  $\text{D}16\text{T}$ ; 2 – Ti; 3 – stainless steel; 4 – square tube; 5 – confusor  $\theta=5^\circ$  b) 1- cylindrical thermalizer; 2 – box-shaped thermalizer; dotted lines corresponded to calculations

The experimental data are shown in Fig.5. Dotted lines correspond to calculations for the diffuse reflection model of gas-surface interaction in dependence of

$$Q_n^* = 2\sqrt{\pi} \frac{V_\infty}{u_2} \frac{B_{n \text{ exp}}}{B_{n \text{ calc}}}$$

The experimental results show that the increase in the gas density in the thermalizer is independent on its geometry, but depends on the gas type and its velocity [12], [18]. It should be noted that the intake flow conditions in VAT-103 differ from real flight conditions. The main difference is divergence of the gas flow in the wind tunnel instead of a uniform flow in the atmosphere.

The calculation was carried out taking into account all gas components; their total density ( $n_{N_2} + n_{O_2} + n_O$ ) is given in the picture. The gas mixture going back into atmosphere consists of molecular nitrogen and molecular oxygen. Atmospheric parameters were taken from CIRA-2012 at the average level of solar activity. As one can see, the gas density in the storage chamber can be increased approximately 300 times as compared to the density of the gas in the atmosphere.

The multi-channel scheme is the potential way for increasing the output channel efficiency. The free molecular flow is characterized by independent boundary conditions at outputs of different channels for flows inside them [19], if the input cross sections do not influence each other (i.e. there is no interference). For example, the input cross sections are in the same plane normal to SC velocity vector. Moreover, all features of the flow in the inlets depend only on their shape, relative length, orientation with respect to SC velocity vector and on the velocity ratio  $S_\infty = V_\infty/u_\infty$ . It is advisable to use not the single channel, but the honeycomb structure for saving the total flow of molecules incoming into the thermalizer [10], [18]. The honeycomb structure is characterized by several advantages with respect to the single channel: it is compact under the same values of gas compression in the thermalizer and the flow rate taking into the thrust unit; it is possible to use the whole volume of the SC midsection for increasing gas intake on contrast to the circular slit structure of the inlet, for example; it is possible to decrease SC drag since it is possible to “hide” its lateral surface behind the input cross section of the inlet.

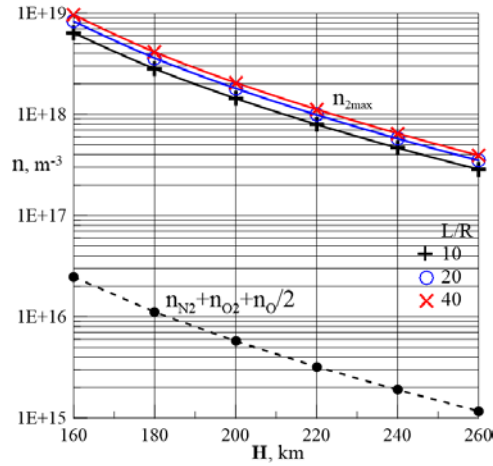


**Fig. 6.** Increase in the density of gas in the thermalizer, depending on the altitude of SC for a cylindrical tube intake

The selection of gas to the thrust unit (Fig. 3) to create a high ion flux, providing compensation for SC aerodynamic braking, change the gas density in a thermalizer. This change can be determined from the basic equation (1). Determine the flow of gas departing to the thrust unit

$$J_{out} = \frac{n_2 U_2}{2\sqrt{\pi}} \rho_{3d} A_3 = J_{\infty} \rho_{1S} - \frac{n_2 U_2}{2\sqrt{\pi}} \rho_{2d} A_2, \quad J_{\infty} = n_{\infty} V_{\infty} A_1. \quad (3)$$

Using (2) and introducing the relative values  $j_{out} = J_{out}/J_{\infty}$ ,  $j_{out\ max} = \rho_{1S}$ , we obtain the throttle characteristic of the air intake

$$\frac{j_{out}}{j_{out\ max}} + \frac{n_2}{n_{2\ max}} = 1. \quad (4)$$

From (4) it follows that as the flow rate increases, the concentration of molecules at the entrance to the accelerating device decreases. The equation (4) — the throttle characteristic — was obtained in [20] for the free-molecular gas flow. To compare the efficiency of air intakes with different geometrical parameters, dependencies  $n_2/n_{2\ max}$  can be built in function of relative flow rate  $j_{out}$ , which for cylindrical intakes are shown in Fig. 7.

The envelope line separates the region of possible parameters on the plane  $(n_2, j_{out})$ . In addition, this line allows to estimate the maximum gas density and the geometric parameters of the intake for a given amount of gas selection. For example, for  $j_{out} = 0.2$  maximum density  $n_{2\ max}/n_{\infty} \approx 220$  and  $L/R \approx 20$ , and for  $j_{out} = 0.4$  —  $n_{2\ max}/n_{\infty} \approx 123$  and  $L/R \approx 10$ .

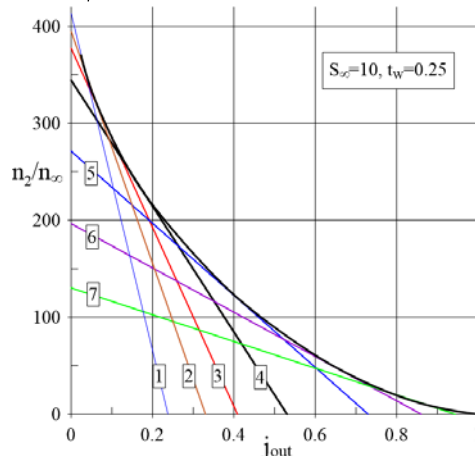


**Fig. 7.** The throttle characteristic of the intake with:  $L/R=60$  (1), 40 (2), 30 (3), 20 (4), 10 (5), 5 (6), 2 (7).

## 5. Models of ABEP thrust unit and their tests

The radio-frequency ion thruster (RFIT) (Fig. 8), which makes it possible to obtain high-velocity ion fluxes of chemically active gases is used as a thrust unit of ABEP. RFIT contains a discharge chamber, inside which the alternating electromagnetic field with frequency of about 2 MHz is generated by an inductor. The propellant in atomic form (traditionally it is xenon) is fed inside the discharge chamber. If there are atoms and electrons inside the discharge chamber, the last ones are accelerated in the alternating electromagnetic field. If accelerated electrons collide with atoms, atoms are ionized. The formed ions are accelerated by electrostatic force and fly out through the perforated electrodes of ion-optical system (IOS) generating the thrust. Electrons from neutralizer are added to the flying out ion flux for compensating the spatial charge of SC. If this scheme is used in ABEP, the propellant is the nitrogen and oxygen mixture.

According to the results of preliminary experimental and theoretical investigations the variant of the prototype of the ABEP thrust unit was chosen (Fig. 9a). The laboratory model of the ABEP thrust unit was developed for power of 1 kW with beam size of 150 mm (Fig. 9b). Under tests the model demonstrates stable operation in the wide range of powers and atmospheric gases flow rates.

Figure 10 depicts the test results for thrust unit model of the ABEP thrust unit. Here vertical blue line corresponds to the concentration in the input flow at the altitude 200 km. Taking into account the WG mass utilization factor, to the left of this line, the thrust unit can work stably and efficiently. Values for thrust and propellant exhaust velocity are presented in Table 1.

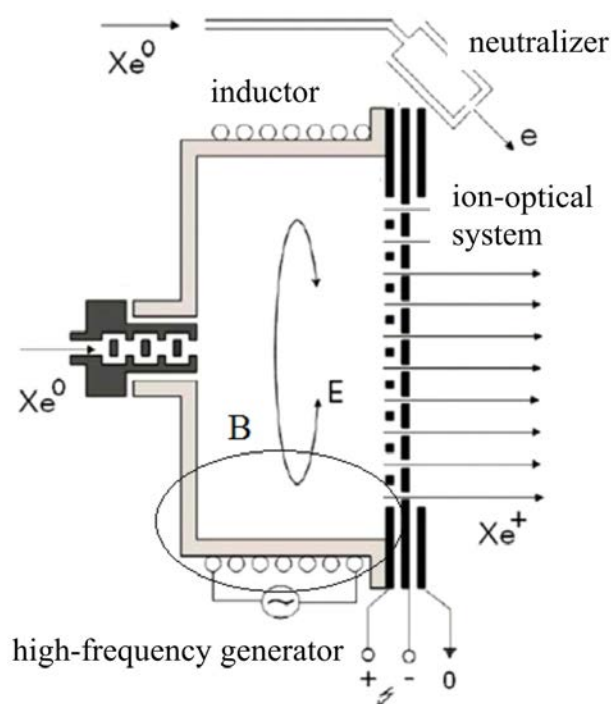


Fig. 8. RFIT block-diagram

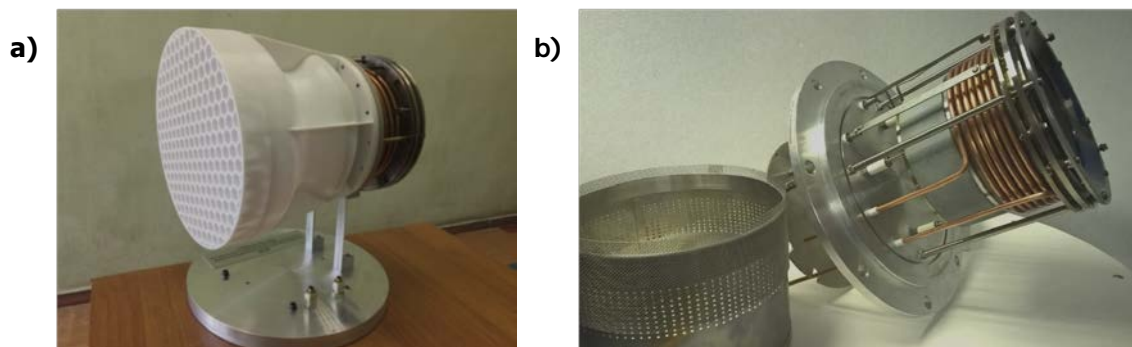


Fig. 9. a) The ABEP prototype, b) the laboratory model of the ABEP thrust unit

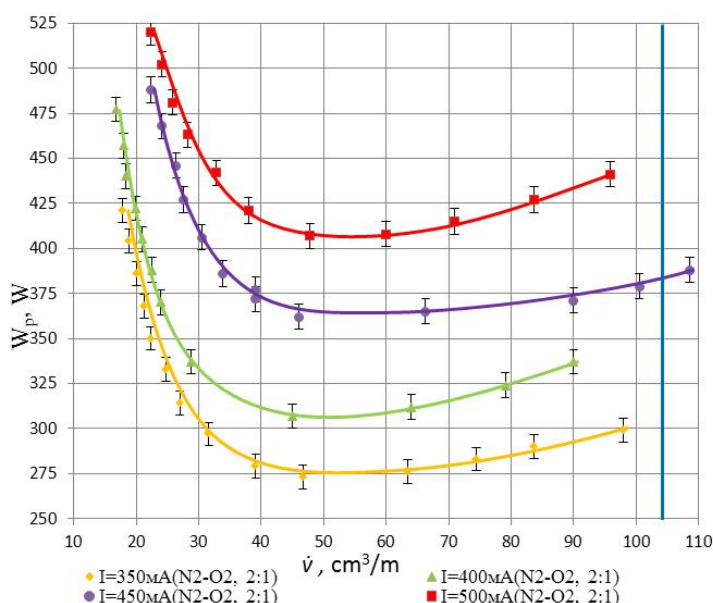


Fig. 10. The relationship between the power consumed by RFIT and propellant flow rate for the laboratory sample of the ABEP thrust unit for atmospheric mixture of nitrogen and oxygen

Table 1. The results of investigation of RFIT, operating with different gases

	Ion current, mA	Propellant			
		Xe	N <sub>2</sub>	O <sub>2</sub>	N <sub>2</sub> + O <sub>2</sub> (2:1)
Exhaust velocity, m/s		42015	128521	120220	124163
Thrust, mN	350	19,3	6,34	6,7	6,6
	400	22,1	7,24	7,7	7,5
	450	24,9	8,15	8,7	8,43
	500	27,7	9	9,6	9,4

## 6. The evaluation of regions of preferable using the ABEP

Comparison of using the ABEP and electric propulsion (EP) for SC maintenance in a low circular orbit was carried out according to the SC mass criterion for a given mass of payload and SC lifetime. Masses of other elements, such as SC structure, navigation, radio-television, and thermal control

systems, etc.; the cross-sectional area  $S$  and the energy efficiency are assumed to be the same for both SC with ABEP and with EP. A solar cell battery was considered as a PS.

Taking into account the assumptions made for estimating the area in which ABEP has an advantage compared to EP, the ratio is obtained

$$\Delta m_{SC} = m_{SCER} - m_{SC EP} = \mu_{EP} \left[ \left( k_{PP} + \frac{k_{SB}}{1 - k_{Cx} \rho V^2} \right) (k_M - 1) \frac{I_{EP}^2}{2\eta_{EP}} + k_{IN} \frac{2I_{EP}}{C_x \rho V^2} - k_T \tau \right] < 0,$$

Where  $m_{SCER}$ ,  $m_{SC EP}$  are the masses of SC with ABEP and SC with EP respectively,  $\mu_{EP}$  is the EP second flow rate,  $I_{EP}$  is the EP specific impulse,  $\eta_{EP}$  is the EP efficiency factor,  $C_x$  is the aerodynamic drag coefficient of SC with EP,  $k_{PP}$  is the specific power plant (PP) mass, equal to the PP mass ratio to the PP power  $W_p$ ,  $k_{SB}$  is the specific SB mass, equal to the ratio of SB mass to the  $W_p$ ,  $k_M$  is the ratio of the thrust powers of EP and ABEP, defined by their WG molar masses ratio,  $k_T = 1 + \delta_T$ ,  $\delta_T$  is the relative mass of WG tank for SC with EP,  $k_{IN}$  is the specific mass of the intake and thermalizer (per unit of the cross-sectional area  $S$ ),  $k_{Cx} = 0.5 k_M I_{EP} / (\sqrt{\pi} S_\infty k_S \eta_{EP})$ ,  $k_S$  is the SB specific area, equal to the ratio of SB area to its power.

Figure 11 shows the areas in which the ABEP has an advantage over the EP with parameters values listed in table 2, depending on the specified lifetime, the orbit altitude, and the material of the intake and thermalizer. The upper limit on the flight altitude of SC with ABEP in Fig. 11 is determined by the level of the required WG concentration in the ABEP ionization chamber for its stable operation. The lower limit on the SC flight altitude is due to the lack of the available power to compensate for the aerodynamic drag.

**Table 2.** Parameters of SC, engines, SB

$I_{EP}$ , m/s	$\eta_{EP}$	$C_x$	$k_{IN}$ , kg/m <sup>2</sup>	$k_{PP}$ , kg/W	$k_S$ , W/m <sup>2</sup>	$k_{SB}$ , kg/W	$k_M$	$k_T$
30000	0.6	2.2	[11.475, 30.645]	0.03	330.0	0.04	2.125	1.1

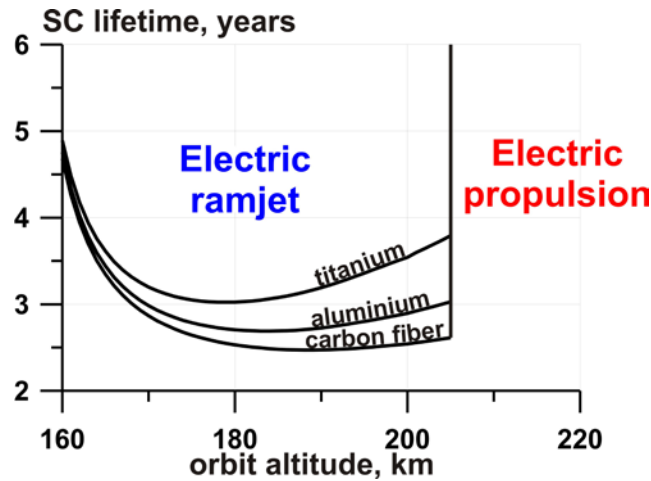


**Fig. 11.** Regions of preferable using ABEP depending on the specified SC lifetime, orbit altitude, and intake and thermalizer material

## 7. The control optimization

The problem of optimizing the ABEP thrust vector control for the fastest change in the orbit parameters is considered. In the problem statement assumptions were made about the negligible changes in the SC mass and the normal aerodynamic force at constant PS power  $W_{in}$  and exhaust velocity  $c$ .

Taking into account the accepted assumptions and the smallness of the disturbing overload, the problem of maximizing the change in orbit parameters was replaced by determining the maximum local efficiency of changing the osculating orbit parameters at each time point. The optimal laws of thrust vector control of  $\mathbf{P}_{opt}$  were determined, which ensure: the maximum rate of change of the apogee radius  $r_a$  at a fixed perigee radius  $r_\pi$  (Problem I)

$$\Phi_I = \left. \frac{dr_a}{dt} \right|_{r_\pi=const} \Rightarrow \max_{\mathbf{P}}$$

the maximum rate of change of the orbit inclination  $i_{orb}$  (Problem II)

$$\Phi_{II} = \left. \frac{di_{orb}}{dt} \right|_{\substack{r_\pi=const \\ r_a=const}} \Rightarrow \max_{\mathbf{P}}$$

Analytical solutions of the problems are obtained. It is shown that the efficiency of using the ABEP to increase the apogee radius varies depending on the position of the spacecraft in orbit (true anomaly

$\nu$ ) within:  $\min_i \frac{dr_a}{dt} = 0$ ,  $\max_i \frac{dr_a}{dt} = \frac{4r_\pi r_a^2 \sqrt{P_{max}^2 + D^2}}{C^3}$ , (where  $D$  is the aerodynamic drag,

$C = |\mathbf{C}| = |\mathbf{r} \times \mathbf{V}|$ ,  $\mathbf{r}$  and  $\mathbf{V}$  are the SC radius-vector and velocity vector respectively) that are reached at apogee and perigee, respectively. The maximum efficiency of the change in inclination is realized on the node line when  $\nu = 2\pi - \omega$ ,  $\pi - \omega$  ( $\omega$  is the argument of perigee), the minimum is when

$$\nu = 3\pi/2 - \omega, \pi/2 - \omega: \max_\nu \left. \frac{di_{orb}}{dt} \right|_{\nu=2\pi-\omega} = \frac{r}{C} \sqrt{P_{max}^2 - D^2}, \quad \min_\nu \left. \frac{di_{orb}}{dt} \right| = 0.$$

In Fig. 12a for an orbit with altitudes of the perigee  $h_\pi = 140$  km and apogee  $h_a = 260$  km, the angle  $\alpha_{opt}$  between the optimum thrust vector  $\mathbf{P}_{opt}$ , and the velocity vector  $\mathbf{V}$ , and the efficiency of changing the apogee radius  $\overline{\frac{dr_a}{dt}}$ , related to its maximum, are shown for different values of exhaust velocity  $c$ . For the same parameters Figure 12b shows the angle  $\varphi_{opt}$  between the thrust vector  $\mathbf{P}_{opt}$

and the orbit plane, and the efficiency of the change in the orbit inclination  $\overline{\frac{di_{orb}}{dt}}$ , referred to its

maximum. The jumps of the angles  $\alpha_{opt}$  and  $\varphi_{opt}$  occur at almost zero thrust  $\overline{P}$  (green curves in the figures) and zero efficiency of changing the parameters of the orbit. The results in fig. 12 were obtained without taking into account the PS power limitation. Figure 13 shows the power  $\overline{W}_p$  required to change the apogee radius  $\Delta \overline{r}_a$ . Obviously, due to the quadratic power dependence on the exhaust velocity, the use of ABEP with a high specific impulse (exhaust velocity) is unprofitable from the point of view of energy supply.

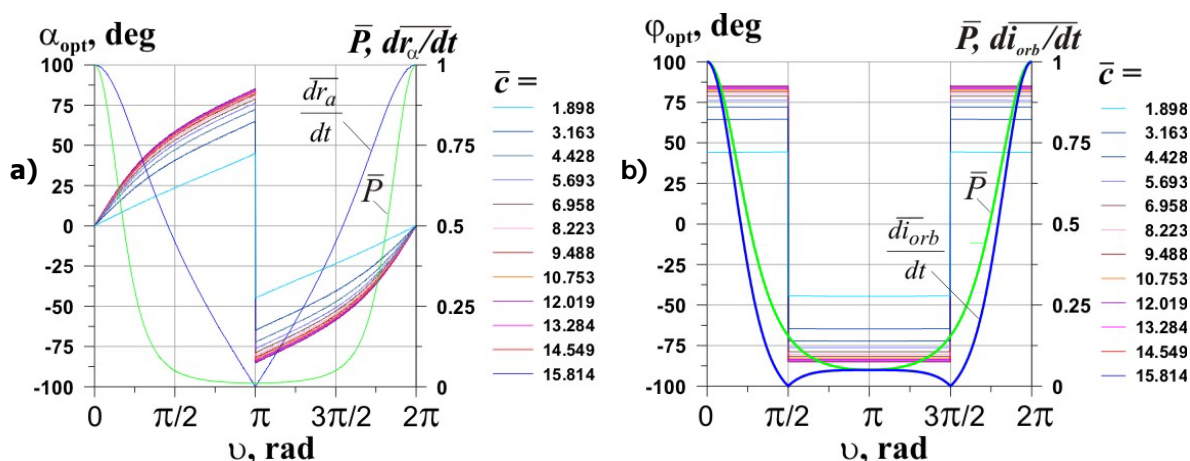


**Fig. 12.** The optimal angles a)  $\alpha_{opt}$  and b)  $\varphi_{opt}$ , and efficiencies of changing the orbit parameters versus true anomaly  $\upsilon$  and dimensionless exhaust velocity  $\bar{c}$

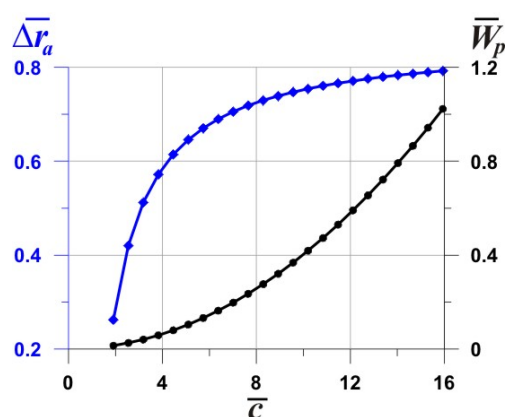


**Fig. 13.** The dimensionless PP power  $\bar{W}_p$  required for realizing apogee radius changes  $\Delta \bar{r}_a$  depending on dimensionless exhaust velocity  $\bar{c}$

## 8. Conclusions

The investigations continue TsAGI's research of electric propulsion, begun in the 60s of the last century, on the new complex technology base.

The possibility of accumulation of the outer rarefied atmosphere for stable long operation of air-breathing electric propulsion at altitudes of 160 – 220 km is confirmed experimentally and by the numerical modeling.

## References

1. Corbett M.H., Edwards C.H. Thrust Control Algorithms for the GOCE Ion Propulsion Assembly / 30th International Electric Propulsion Conference. - Florence, Italy, September 17-20, 2007. -IEPC-2007-210.
2. Важенин Н.А., Обухов В.А., Плоких А.П., Попов Г.А. Электрические ракетные двигатели космических аппаратов и их влияние на радиосистемы космической связи. – М.: ФИЗМАТЛИТ (2012) (Bazhenin, N.A., Obukhov, V.A., Plokhikh, A.P., and Popov, G.A., Electric propulsion thrusters for the spacecrafts and their impact to radio systems of space communication. – Moscow: FIZMATLIT (2012)).
3. Киселёв К.В., Медведков И.А., В.П. Ходненко, и др. Результаты лётных испытаний корректирующей двигательной установки с двигателем СПД-50 на борту космического аппарата типа «Канопус-В» // Вопросы электромеханики. Труды ВНИИЭМ. – М.: ОАО «Корпорация «ВНИИЭМ», Т. 137, № 1, С. 7–14 (2013) (Kiselev, K.V., Medvedkov, I.A.,

- Khodnenko, V.P., et al. The results of flight tests of correcting power plant with SPT-50 onboard the spacecraft of "Kanopus-V" type, *Vopr. Elektromekhan. Trudy VNIIEМ*, Vol. 137, No. 1, pp. 7-14 (2013)).
4. Гродзовский Г.Л., Иванов Ю.Н., Токарев В.В. Механика космического полета с малой тягой. М.: Наука, 1966 (Grodzovsky G.L., Ivanov Y.N., Tokarev V.V. Mechanics of space flight with low thrust. M.: «Nauka». (1966)).
  5. Балаев Н.Ф., Гродзовский Г.Л., Данилов Ю.И. и др. Научные результаты полетов автоматических ионосферных лабораторий «Янтарь» // Ученые записки ЦАГИ, Т. II, №2, стр. 58-65, (1971) (Balaev N.F., Grodzovsky G.L., Danilov Yu.I., et al. Scientific results of flights of automatic ionospheric laboratories "Yantar" // Uch. Zapiski TsAGI, Vol. II, No. 2, pp. 58-65 (1971)).
  6. Demetriades S.T. A novel system for space flight using a propulsive fluid accumulator. 1. *British Interplanetary Society*, Vol. 17, № 5, 1959.
  7. Kanev S.V., Petukhov V.G., Popov G.A., Khartov S.A. Electro-rocket ramjet thruster for compensating the aerodynamic drag of a low-orbit spacecraft / *Russian Aeronautics (Iz.VUZ)*, 2015, Vol. 58, No. 3, pp. 286-291.
  8. Ерофеев А.И., Никифоров А.П., Попов Г.А., Суворов М.О., Сырин С.А., Хартов С.А. Разработка воздушного прямоточного электрореактивного двигателя для компенсации аэродинамического торможения низкоорбитальных космических аппаратов // Вестник «НПО имени С.А. Лавочкина», 2016, № 3, С. 104-110 (Erofeev, A.I., Nikiforov A.P., Popov G.A., Suvorov M.O., Syrin S.A., Khartov S.A., Development of air-electrorocket ramjet for compensating of low-orbit spacecrafts aerodynamic drag, Vestnik NPO imeni S.A. Lavochkina, No. 3, pp. 104-110 (2016)).
  9. DiCara D., Gonzalez del Amo J., Santovincenzo A., et al. RAM Electric Propulsion for Low Earth Orbit Operation: an ESA study / 30th International Electric Propulsion Conference, Sept. 2007, IEPC-2007-162.
  10. Barral S., Cifali G., Albertoni R., Andrenucci M., Walpot L. Conceptual Design of an Air-Breathing Electric Propulsion System / 34th International Electric Propulsion Conference, Kobe, Japan, 04-10 July 2015, IEPC-2015-271.
  11. Cifali G., Andreussi T., Giannetti V., Leporini A., Rossodivita A., Andrenucci M., Barral S., Longo J., Walpot L. Experimental validation of a RAM-EP concept based on Hall effect thruster technology // Proc. of Space propulsion conf. 2016, Rome, Italy, 2- 6 May 2016. - SP2016-3125202.
  12. Erofeev A.I., Nikiforov A.P., Plugin W.W. Experimental studies of the air intake in a free-molecular gas flow // *TsAGI Sci. J.*, Vol. XLVIII, No 3, pp. 56-69 (2017).
  13. Filatyev A.S., Erofeev A.I., Nikiforov A.P., Golikov A.A., Yanova O.V. Comparative Evaluation of the Applicability of Electrical Ramjets // Proceedings of the 58th Israel Annual Conference on Aerospace Sciences, Tel-Aviv & Haifa, Israel, March 14-15, 2018.
  14. Golikov A.A., Yanova O.V. Spacecraft Safety in Very Low Earth Orbits // Proceedings of the 69th International Astronautical Congress, Bremen, Germany, 01-05 October 2018, Paper IAC-18-D5.1.5.
  15. Marov M.Ya., Filatiev A.S. Integrated research of electrojet engines in Earth's ionosphere: To the 50-th anniversary of State Program "Yantar". *Cosmic Research*, Vol. 56, No. 2, pp. 123–129 (2018).
  16. Кузнецов Ю.Е., Флакман Я.Ш. Влияние закона отражения молекул от стенок канала на характеристики свободномолекулярного воздухозаборника // Ученые записки ЦАГИ, Т. VII. №4. 1976. С. 148-152. (Kuznetsov Yu.E., Flaksman Ya.Sh. The Influence of the law of molecule reflection from channel walls on characteristics of the free molecular intake // Uchenye zapiski, Vol. VII, No. 4, pp. 148-152 (1976)).
  17. Shabshelowitz A. Study of RF plasma technology applied to air-breathing electric propulsion. Univ. of Michigan. 2013, 188

18. Кузнецов Ю.Е., Флакман Я.Ш. Влияние формы поперечного сечения канала на характеристики свободномолекулярных воздухозаборников / Труды ЦАГИ. Вып. 1863. С. 25-29 (1977) (Kuznetsov, Yu.E., and Flaksman, Ya.Sh. How the shape of transversal cross section of the channel influences onto performances of free molecular inlets, Trudy TsAGI, issue 1863, pp. 25–29 (1977)).
19. Кошмаров Ю.А., Рыжов Ю.А. Прикладная динамика разреженного газа. – М.: Машиностроение, 1977. – 184 с. (Koshmarov, Yu.A., Ryzhov, Yu.A. Applied rarefied gas dynamics, M.: Mashinostroenie (1977)).
20. Богомазов В.И., Кузнецов Ю.Е., Носик В.А. О характеристиках цилиндрических воздухозаборников в свободномолекулярном потоке // Ученые записки ЦАГИ, Т. I. №5. 1970. С.101-104 (Bogomazov, V.I., Kuznetsov, Yu.E. On the characteristics of cylindrical air intakes in the free molecular flow // Uchenye zapiski, Vol. I, No. 5, pp. 101-104 (1970)).